Science Translational Medicine
AAAS

www.sciencetranslationalmedicine.org/cgi/content/full/11/477/eaat7973/DC1

Supplementary Materials for

A biologic scaffold–associated type 2 immune microenvironment inhibits tumor formation and synergizes with checkpoint immunotherapy

Matthew T. Wolf, Sudipto Ganguly, Tony L. Wang, Christopher W. Anderson, Kaitlyn Sadtler, Radhika Narain, Christopher Cherry, Alexis J. Parrillo, Benjamin V. Park, Guannan Wang, Fan Pan, Saraswati Sukumar, Drew M. Pardoll, Jennifer H. Elisseeff*

*Corresponding author. Email: jhe@jhu.edu

Published 30 January 2019, *Sci. Transl. Med.* **11**, eaat7973 (2019)
DOI: 10.1126/scitranslmed.aat7973

The PDF file includes:

Other Supplementary Material for this manuscript includes the following:

(available at www.sciencetranslationalmedicine.org/cgi/content/full/11/477/eaat7973/DC1)

Table S1 (Microsoft Excel format). Sorted T cell gene expression data.
Table S2 (Microsoft Excel format). Sorted macrophage gene expression data.
Table S5 (Microsoft Excel format). Primary data.

Materials and Methods

Injectable biomaterials and reagents. Lyophilized urinary bladder matrix (UBM) particulate was obtained from ACell Inc. UBM is produced in a facility adhering to good manufacturing practices (GMP) and is terminally sterilized for clinical or pre-clinical application. The proteomic composition of UBM has been described previously (*19*). Synthetic particulate material controls include alum (endotoxin free 2% aluminum hydroxide gel, Alhydrogel, InvivoGen) and mesoporous silica SBA-15 (<150 μm particle size, pore size 8 nm, Sigma-Aldrich). ECM particles from other tissue sources were compared to UBM: porcine small intestinal submucosa (SIS) and human acellular adipose tissue ECM (AAT). SIS was prepared as previously described (*36*) and represents a biologic scaffold material with nearly 30 years of investigation. The jejunum of porcine intestine was obtained from a local abattoir (Wagner's Meats LLC, Mt. Airy, MD), extensively rinsed with the water, and the lumen opened into a flat sheet. The majority of the mucosa layer and the entire serosa and muscularis externa layers were then mechanically removed from the intestine leaving the submucosa, muscularis mucosa, and stratum compactum layers. This tissue was rinsed with deionized water and treated with 0.1% (w/v) peracetic acid/4% (v/v) ethanol for 2 hours with strong agitation. The resulting SIS sheets were rinsed extensively with alternating PBS and deionized water, lyophilized, and micronized into particles using a cryogenic mill (SPEX SamplePrep). Human AAT was prepared from cadaveric subcutaneous adipose tissue obtained from a tissue bank (LifeNet Health, Virginia Beach, VA) as previously described with modification (*37*). AAT is a biologic scaffold material currently undergoing clinical trials (ClinicalTrials.gov, NCT Identifiers: NCT03544632 & NCT02817984). In brief, excess lipids were extruded from adipose tissue by mechanically pressing several times with a steel mesh, followed by extensive rinsing with PBS. Adipose tissue was then treated with 3% peracetic acid (w/v) for 3 hours at 37°C with agitation followed by extensive rinsing with PBS and HEPES buffer. Washed tissue was decellularized with 0.5% Triton X-100/0.2% EDTA for 16 hours with agitation followed by rinsing with deionized water. The resulting AAT was homogenized with a knife-mill (Retsch, Haan, Germany), lyophilized, and further micronized into particles using a cryogenic mill.

IL-4 complex (IL-4c) was prepared by mixing 20 μg of recombinant murine IL-4 (PeproTech) with 100 μg of anti-IL-4 monoclonal antibody (clone 11B11, BioXcell) for 20 minutes on ice. This corresponds to a 1:5 weight ratio of IL-4:anti-IL-4 (equivalent to a 1:2 molar ratio). IL-4c was mixed with UBM at least 30 min before injection.

Mice. Wild type (WT) C57BL/6 and balb/c mice were obtained from Charles River Laboratories or The Jackson Laboratories. Lymphocyte deficient *Rag1*$^{-/-}$ mice (B6.129S7-Rag1^{tm1Mom}/J) and EGFP/IL-4 reporter mice (4get mice, C.129-Il4^{tm1Lky}/J) were obtained from Jackson Laboratories. Each experiment used female aged matched mice raised in the same facility.

Cell culture. B16-F10 (CRL-6475) melanoma, CT26 (CRL-2638) colorectal carcinoma, and 4T1 mammary carcinoma (CRL-2539) tumor cell lines were obtained from the American Type Cell Culture Collection (ATCCC). Luciferase transduced B16-F10 cells were obtained from Perkin Elmer, Inc. All cell lines were grown in DMEM media supplemented with 10% heat-inactivated FCS (Hyclone), 2 mM L-glutamine, 100 U/ml penicillin G, and 100 μg/ml streptomycin (Hyclone).

In vitro UBM biocompatibility. The effect of UBM particles on B16-F10 melanoma adhesion and viability was evaluated in vitro. Glass coverslips were coated with 0.4 mg/cm^2 UBM or Type I collagen (Sigma-Aldrich) as previously described (*38*). B16-F10 melanoma cells were seeded in triplicate on coated and uncoated 12 mm coverslips at a density of 15,000 cells/cm^2 and given 1.5 hours to attach. Non-adherent cells were removed with 3 PBS washes and the remaining cells incubated with Calcein-AM viability dye (Thermo Fisher) for 20 min. Coverslips were then imaged for viable cell adhesion and the number of stained cells counted.

Scanning electron microscopy (SEM). The topography of UBM particles before and after implantation was characterized by SEM. Post-implantation UBM was carefully dissected from mice and fixed in 2.5%

glutaraldehyde, 3 mM MgCl, 0.1M cacodylate buffer (pH 7.2) for 24 hours at 4°C with agitation. Samples were rinsed three times with cacodylate buffer and further fixed with 1% osmium tetroxide in cacodylate buffer for 1 hour at room temperature. Samples were rinsed with water and dehydrated with a graded series of ethanol (30%, 50%, 70%, 90%, and three times in anhydrous 100% ethanol) for 15 min with agitation during each step. Samples were dried with a 1:1 solution of hexamethyldisilizane (HMDS):100% ethanol and two additional changes of 100% HMDS for 15 min each followed by overnight dessication. Dried implants and pre-implant particles were sputter coated with 10 nm gold/palladium alloy and imaged using a LEO (Zeiss) field-emission SEM with 1kV accelerating voltage.

Subcutaneous tumor formation. The syngeneic cancer lines B16-F10 melanoma, CT26 colorectal carcinoma, and 4T1 mammary carcinoma were implanted subcutaneously in 7-8 week old female C57BL/6 (for B16-F10 cells) or balb/c mice (for CT26 and 4T1 cells), with and without UBM. Cells were used within the same two passages for all experiments. UBM particles were hydrated with phosphate buffered saline and then thoroughly mixed with cell suspension to a final concentration of 50 mg UBM (dry wt)/ml. The right flanks of mice were shaved, disinfected with 70% ethanol, and injected with $1x10^5$ cancer cells suspended in 100 µl of saline or UBM (5 mg of UBM particles per injection). This amount was determined from a dose response study using 0, 12.5, 25, and 50 mg UBM/ml suspension (**Fig. S14**). Tumor dimensions were monitored by external measurements using digital calipers. Tumor volume was calculated by the following equation where L is the tumor length (larger dimension) and W is the width (smaller dimension):

$$Tumor\ volume\ = \frac{\pi}{6}\ (L\ \times\ W^2)$$

Mice were sacrificed by carbon dioxide asphyxiation once tumors grew to 19.5-20 mm in any dimension according to Johns Hopkins Animal Care and Use Committee policy. Survival was defined as the number of days before reaching this maximum allowable size before sacrifice.

Mice that rejected the initial cancer cell injection were rechallenged with the same cell line to determine whether long-term protection had been established. Mice were rechallenged with the same cancer cell line in saline (10^5 cells, a cell does that results in 100% tumor formation frequency in naïve mice) at least 60 days following the initial injection. Rechallenge injections were performed in the same flank as the initial cancer cell injection. Tumor formation and growth was monitored as described above.

In vivo bioluminescence imaging of tumors. Live animal bioluminescence imaging was conducted to monitor cancer cell engraftment and growth before palpable tumors had formed using the IVIS Spectrum In Vivo Imaging System (Perkin Elmer). Firefly luciferase expressing B16-F10 cells were injected with saline or UBM particle suspension as described above and imaged after 1, 3, and 5 days post implantation. Each mouse was intraperitoneally injected with 150 mg/kg of D-Luciferin/K^+ (XenoLight, Perkin Elmer) 15 minutes prior to imaging, anesthetized via isofluorane inhalation, and imaged with a range of exposure times. The injection site (right flank region) of each mouse was analyzed for normalized luminescent flux (photons/s) to determine cancer burden. WT B16-F10 cells delivered with saline or UBM (N=2) were used as negative controls to confirm specificity of the bioluminescent signal.

Orthotopic breast cancer tumor formation and resection model. 4T1 mammary carcinoma tumors were resected from the mammary fat pad of 8 week old female balb/c mice and treated with UBM to determine the effect of biologic scaffold implantation on tumor recurrence and metastasis. Mice were anesthetized and the surgical site shaved/disinfected. A 1 cm skin incision was made to expose the right flank for injection with 1 x 10^6 4T1 cells (expressing firefly luciferase) suspended in 50 µl of MatriGel (BD Biosciences) directly into the right abdominal mammary fat pad. The incision was closed with single interrupted Vicryl sutures, and the animals allowed to ambulate normally. Once 4T1 tumors grew to approximately 1 cm in greatest dimension (day 10), a second surgery was performed to remove the tumor bulk. Immediately following removal of the entire visible tumor mass, 0.2 ml of a 100 mg/ml UBM particle suspension or saline alone was injected into the resection bed. Tumor volume at the primary

resection site was monitored by external measurement. Bioluminescence imaging was performed after 7 days as described above to quantify lung metastasis and to confirm recurrence at the primary resection site.

B16-F10 Tumor histology and immunolabeling. Histologic analysis of tumors was conducted 7 days post-injection and also after tumors had grown to a volume of 200 mm^3. Whole tumors and UBM were explanted, fixed for 2-3 days in neutral buffered formalin, and dehydrated with a graded series of ethanol: 70%, 80%, 95% (2x), and 100% (3x) for at least 1 hour each. Tumors were cleared with 3x 45 min changes of Xylene and then infiltrated with several changes of paraffin wax. Embedded tumors were cut into 5 µm sections for H&E staining or immunofluorescent (IF) histologic staining. IF staining was conducted to characterize T cell, B cell, and macrophage infiltration and phenotype. Sections were deparaffinized and underwent antigen retrieval in citrate buffer (0.01 M citrate, pH 6) for 20 minutes at 95-98°C in a vegetable steamer. Nonspecific binding was blocked for 1 hour using 4% normal goat serum (Vector labs)/1% bovine serum albumin (Sigma), and then incubated with primary antibodies diluted in blocking buffer overnight at 4°C. A full list of primary antibodies and dilutions are provided in **table S3**. Following washing, fluorescent conjugate secondary antibodies were applied for 1 hour at room temperature: goat anti-rat Alexa Fluor-488 and goat anti-rabbit Alexa Fluor-568 (Thermo Fisher). Background fluorescence was quenched by incubating in Sudan Black B (Sigma) in 70% ethanol for 20 min. Sections were rinsed with water, counterstained with DAPI, coverslipped, and imaged. Spleen tissue was processed and stained as described for tumors.

Flow cytometry and cell sorting from tumors and lymphoid tissues. Infiltrating immune cells in B16-F10 tumors delivered with UBM or saline were characterized by flow cytometry using the antibodies and fluorescent dyes listed in **table S4**. All flow cytometry data was collected using a BD LSR II flow cytometer or a BD FACSAria II, and analyzed using FlowJo software (Tree Star).

Explanted tissues were finely minced in RPMI media and digested with 0.5 mg/ml Liberase TL (Roche) and 0.2 mg/ml DNAse I (Roche) for 45 minutes at 37°C with agitation. The digested tissue was then passed through a 100 μm cell strainer and washed. Small tumors at the 7 day time point were additionally passed through a 70 μm cell strainer and proceeded directly to staining. Larger tumors at the 14 day time point or later underwent density separation using a Percoll gradient (GE Healthcare Life Sciences) to remove excess necrotic cells and debris. One part 10X PBS was added to 9 parts Percoll (1.13 g/ml) to create a 100% Percoll solution, which was then diluted to 80%, 40%, and 20% solutions with PBS. The filtered cell suspension was washed and suspended in 4 ml 80% Percoll, which was subsequently layered with 4 ml of 40% Percoll, and then 3 ml of 20% Percoll above it. Tubes were centrifuged at 1,000 g for 20 min at room temperature and the resulting interfacial layer between the 80% and 40% layers collected for staining. Lymphoid tissues (lymph node and spleen) were harvested, diced, and digested with 0.25 mg/ml Liberase TL (Roche) and 0.2 mg/ml DNAse I (Roche) for 25 minutes at 37°C with agitation. Lymphoid suspensions were filtered through a 100 μm cell strainer, washed, and proceeded directly to cell staining.

Surface staining for flow cytometry was conducted in round bottom 96-well plates on ice and in the dark. Viability staining was conducted for 20 min, followed by a surface staining cocktail for 45 min on ice. Non-specific binding was blocked by anti-CD16/32 during surface staining. T cell surface staining consisted of Viability-Aqua, CD45-PerCP/Cy5.5, CD19-PE, CD3-AF488, NK1.1-APC, CD4-PE/Cy7, CD8-AF700, CD62L-APC/Cy7, CD44-BV605. Myeloid surface staining consisted of Viabilitiy-eFluor780, CD45-BV605, CD11b-AF700, MHCII-AF488, Siglec F-PE/CF594, Ly6C-PerCP/Cy5.5, Ly6G-Pacific Blue, F4/80-PE/Cy7, CD11c-APC, CD206-PE, CD86-BV510. Samples were fixed with Cytofix/Cytoperm (BD) for 25 min on ice for analysis the next day, or used immediately for cell sorting experiments. Small saline tumors (7 day time point) were pooled prior to sorting to increase immune cell yield. All samples were stored in PBS buffer with 2.5 mM EDTA and passed through a 40 μm cell strainer before flow cytometry analysis.

Cells isolated for intracellular cytokine staining experiments were stimulated for 5 hours at 37°C in a cell stimulation cocktail with transport inhibitors (eBioscience): phorbol 12-myristate 13-acetate (PMA), ionomycin, brefeldin A, and monensin in RPMI media supplemented with 10% FBS, 2 mM glutamine, 1% non-essential amino acids (Gibco), 20 mM HEPEs buffer, 1 mM sodium pyruvate, and 55 µM 2-mercaptoethanol. Cells were then placed on ice, washed, and stained with Viability-Aqua followed by surface staining: CD45-PerCP/Cy5.5, CD3-AF488, CD4-PE/Cy7, CD8-AF700. Cells were fixed and permeabilized for 25 min on ice with Cytofix/Cytoperm and washed with Perm/Wash buffer (BD Biosciences). Intracellular staining was then conducted using antibodies diluted in Perm/Wash buffer for 45 min on ice, followed by washing in Perm/Wash buffer. The following antibodies were used for intracellular staining: FoxP3-Pacific Blue, IL-4-PE, IFNy-BV605.

Some results were normalized by tumor size (cells/mm^3). Viable cell counts were obtained after isolation using a hemocytometer and Trypan blue exclusion before flow cytometry staining. The total number of viable of cells within a cell population were calculated from flow cytometry analysis and hemocytometer counts, and then divided by external tumor volume.

$CD4^+$ T cell adoptive transfer in $Rag1^{-/-}$ mice. The role of $CD4^+$ T cells in the UBM microenvironment was assessed by repopulating *$Rag1^{-/-}$* mice (which lack mature T cells and B cells) with purified $CD4^+$ T cells. Pooled spleens and lymph nodes from 5 week old female WT C57BL/6 mice were harvested and prepared as a single cell suspension using the gentleMACS automated tissue dissociator (Miltenyi). Tissue was digested using the manufacturer's enzyme mix and pre-programmed spleen dissociation cycle for 15 min at 37°C. $CD4^+$ cells were isolated by negative selection via magnetic activated cell sorting (MACS, Miltenyi) following the manufacturer's instructions. In brief, cells were incubated with biotinylated antibodies against CD8a, CD11b, CD11c, CD19, CD45R (B220), CD49b, CD105, MHC Class II, Ter-119, and TCRγ/δ, and reactive cells removed by binding to magnetic beads. The purity of the cell suspension was verified with flow cytometry using the following panel: Viability-Aqua, CD45-PerCP/Cy5.5, CD19-PE, CD3-AF488, CD4-PE/Cy7, CD8-AF700 with non-specific binding blocked by

anti-CD16/CD32. Purified $CD4^+$ T cells were transferred to 5 week old *Rag1*$^{-/-}$ mice by tail vein injection (4 million viable cells per mouse). Repopulation was verified 12 days later by flow cytometry. Peripheral blood was collected EDTA solution, red blood cell lysis performed, and stained for the same lymphocyte markers as above. CD4 repopulated *Rag1*$^{-/-}$ mice, *Rag1*$^{-/-}$ mice, and WT mice were challenged with B16-F10 cells with and without UBM 17 days after repopulation.

NanoString gene expression analysis. $CD3^+$ T cells and $F4/80^+$ macrophages were sorted by flow cytometry (**fig. S15**) for NanoString analysis with the following marker panel: Viability-eFluor780, CD45-BV605, CD11b-AF700, CD3-APC, F4/80-PE/Cy7. Sorted cells were analyzed for gene expression using the NanoString Pan Cancer Immune Profiling Panel (XT-CSO-MIP1-12, NanoString Technologies, Inc.). Cells were sorted directly into RLT lysis buffer with 2-mercaptoethanol for RNA purification using the RNEasy micro kit (Qiagen). RNA concentration was fluorometrically quantified using the Qubit RNA HS Assay Kit (Thermo Fisher). For $F4/80^+$ macrophages, 25 μg of RNA was added to a barcoded probeset mixture, and hybridized for 18 hours at 65°C. $CD3^+$ T cells underwent 5 rounds of pre-amplification with the Low RNA Input Kit (PP-MIP1-12, NanoString) followed by a 20 hour hybridization at 65°C. All hybridized samples were processed using a NanoString Prep Station operating under high sensitivity mode, and mRNA target transcripts counted using the nCounter digital analyzer system (NanoString). Data was analyzed using nSolver software (v3.0, NanoString) and complete data sets are presented in **tables S1 & S2**. Gene expression for each sample was normalized to the geometric mean of the reference genes: *Oaz1*, *Hprt*, *Polr2a*, *Sdha*, *Hdac3*, and *Alas1* for $F4/80^+$ macrophages, and *Oaz1*, *Hprt*, *Polr2a*, and *Ppia* for $CD3^+$ T cells. Reference genes were selected for stability across conditions.

Differentially expressed genes in sorted macrophages were categorized as M1 or M2 polarized by comparing to a previously published transcriptomic analysis of in vitro macrophage polarization via RNA-sequencing (*25*). This permits M1/M2 designation in an unbiased fashion. M2 genes were defined as those with significantly greater expression with M2 stimulation (IL-4) compared to M1 stimulation

(lipopolysaccharide and IFNγ). Genes that were not significantly regulated in this published dataset were examined via a manual literature search for M1 or M2 associations, and were classified as "unassociated" if no M1 or M2 consensus was found. Angiogenic, complement pathway, and major histocompatibility genes were consolidated and placed into separate lists as these genes behaved as discrete gene sets. The remaining genes with the 50 largest absolute fold changes compared to saline are displayed. All genes were color coded by their polarization bias: M1 associated (red), M2 associated (green), or unassociated (grey).

Macrophage depletion with clodronate liposomes. Circulating macrophage progenitors were partially ablated by systemic administration of clodronate liposomes (5 mg/ml, clodronateliposomes.com) to determine the role of macrophages in the UBM and tumor microenvironments. Clodronate loaded liposomes or PBS loaded controls (1 mg liposome/20 g mouse) were injected intraperitoneally four and two days prior to cancer cell implantation. The depletion was maintained every other day thereafter until sacrifice (**Fig. S8**). To verify depletion, peripheral blood was collected into EDTA solution and red blood cell lysis performed (Ammonium-Chloride-Potassium lysis buffer) followed by flow cytometry analysis using the following panel: Viabilitiy-eFluor780, CD45-BV605, CD11b-AF700, Ly6C-PerCP/Cy5.5, Ly6G-Pacific Blue, F4/80-PE/Cy7 with nonspecific binding blocked with anti-CD16/32.

Acellular material implantation for tracking IL-4 expression in 4get mice. UBM, alum, or saline alone (without B16-F10 cells) were injected subcutaneously into the flank of 8 week old female 4get mice or WT balb/c mice. 4get mice (Jackson Labs) have a bicistronic IRES-EGFP reporter cassette inserted between the translational stop codon and the 3' UTR of the interleukin 4 gene (IL-4). Both the material implant and the draining lymph node were analyzed for IL-4-EGFP expression by flow cytometry after 7 days using the following panel: Viabilitiy-eFluor780, IL-4-EGFP, CD45-BV605, CD11b-AF700, Siglec F-PE/CF594, Ly6C-PerCP/Cy5.5, Ly6G-Pacific Blue, F4/80-PE/Cy7, CD3-APC, CD19-PE with

nonspecific binding blocked with anti-CD16/32. WT mice were injected with material to determine EGFP signal specificity and gating.

Checkpoint blockade immunotherapy following UBM implantation. B16-F10 cells were injected with saline or UBM in 7-8 week old female C57BL/6 mice as described above. Eight days following implantation, monoclonal antibodies blocking either PD-1 (clone RMP1-14, InVivoPlus grade, BioXCell), PD-L1 (clone 10F.9G2, InVivoPlus grade, BioXCell), or PD-L2 (clone TY25, InVivoMab grade, BioXCell) were delivered intraperitoneally at 5 mg/kg body weight. Checkpoint blocking antibodies were delivered every 3 days for a total of 4 treatment doses. Tumor volume and survival were monitored. IgG2a (clone 2A3, InVivoPlus grade, BioXCell) and IgG2b (clone LTF-2, InVivoPlus grade, BioXCell) isotype controls were delivered using the same schedule (N = 5 for each isotype which were then pooled for analysis).

Delayed UBM delivery was performed in combination with anti-PD-1 to test the effect of UBM on established cancer cells. B16-F10 cells were first injected subcutaneously into the right flank of 7-8 week old female C57BL/6 mice and the skin over the injection site labeled with a marker. One day later, after cells had engrafted in the subcutaneous space, 200 µl of UBM particles (50 mg/ml) or saline was injected in the same approximate area. Four days after UBM or saline injection (day 5 after B16-F10 implantation), anti-PD-1 monoclonal antibody or isotype control was delivered following the same dosing schedule as above (5 mg/kg body weight, 4 injections 3 days apart). Tumor volume and survival were monitored.

The initial B16-F10 cell dose was titrated to model different residual cancer burdens after resection. Female C57BL/6 mice were injected with saline or UBM and a range of B16-F10 cell doses (1 x 10^3, 10^4, 10^5, or 10^6 cells), followed by anti-PD-1 treatment 8 days later (5 mg/kg body weight, 4 injections 3 days apart). Tumor volume and survival were monitored.

Association between melanoma patient survival and the UBM immune gene signature using The Cancer Genome Atlas (TCGA). NanoString gene expression data from sorted macrophages and T cells were compared to melanoma patients to find similarities to the UBM microenvironment. The results are based upon data generated by the TCGA Research Network: http://cancergenome.nih.gov/. The TCGABiolinks R package was used to obtain relevant data from the TCGA database. Patient FPKM gene expression data was obtained with GDCquery using the harmonized database. Likewise, indexed clinical data files were obtained for all patients with gene expression data (where available) usingGDCquery_clinic. FPKM values were log-normalized and each gene subsequently Z scored across all patients. A UBM immune gene signature was defined as genes that were significantly upregulated in UBM-associated macrophages and T cells compared to TAMs and TILs, respectively. A gene expression enrichment score was calculated for each patient using this gene signature as previously described (*39*). UBM immune signature genes were ordered by z-score for each patient, and the immune enrichment score calculated as the sum of ranks for each gene in the set normalized to the highest score. Higher scores indicate higher expression of genes in the UBM immune gene signature. Finally, patients were evenly divided into expression categories based on their enrichment scores (lowest third, middle third, highest third). Kaplan-Meier survival analysis was performed for each expression category using the corresponding patient survival data in the TCGA database.

Supplementary Figures

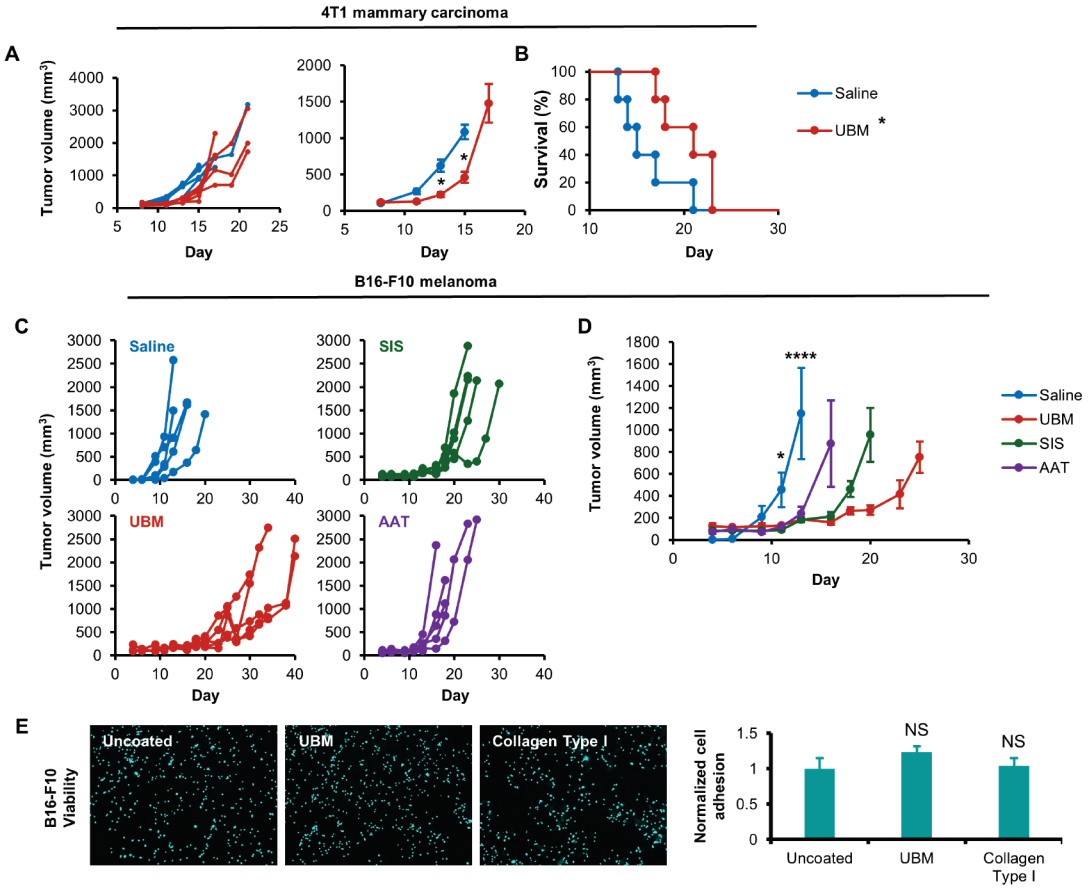

Fig. S1. Biologic scaffolds from different tissue sources inhibit tumor formation but do not affect cancer cell viability. (**A**) Individual tumor growth curves, mean tumor volume, and (**B**) survival after subcutaneous delivery of 4T1 cells with UBM particles or saline. (N=5, mean ± SE). (**C**) Individual B16-F10 tumor growth curves and (**D**) mean tumor growth when implanted with saline or ECM particles derived from porcine UBM, porcine small intestinal submucosa (SIS), or human acellular adipose tissue (AAT). (N=5, mean ± SE). (**E**) B16-F10 cell adhesion and viability in vitro. B16-F10 cells were seeded on glass coverslips coated with UBM particles or bovine Type I collagen for 1.5 hours followed by viability staining with Calcein-AM. (N=3 coverslips, N=3 fields of view, mean ± SE). (**Statistics**) Tumor volume: * $P < 0.05$, **** $P < 0.001$ for any ECM vs saline. Two-way repeated measures ANOVA with post-hoc Tukey test at each time point before sacrifice. Survival: * $P < 0.05$, log-rank test with the Sidak correction. Cell viability: NS, not significant $P > 0.05$, Student's *t* test to uncoated coverslips.

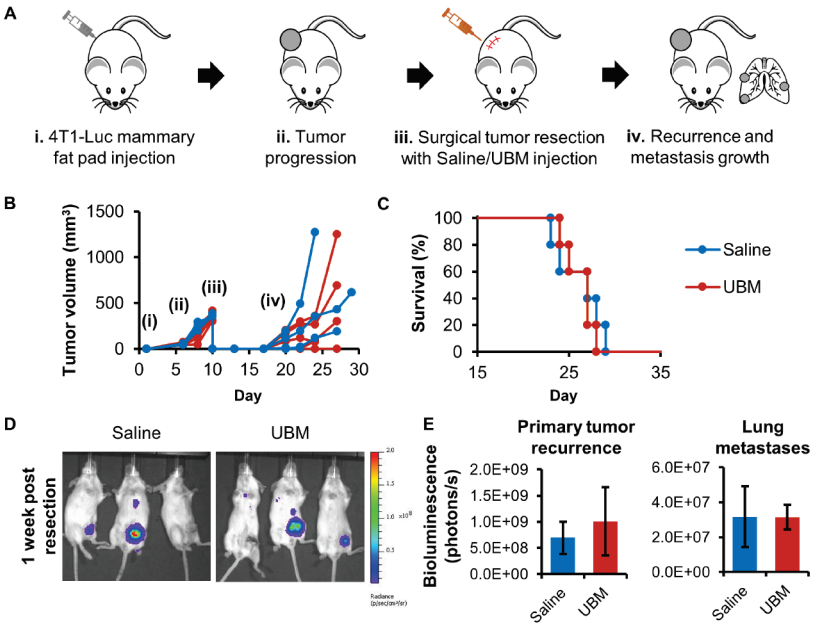

Fig. S2. UBM implantation does not promote tumor growth in an orthotopic breast cancer resection model. (**A**) Schematic of the breast cancer resection model: (**i**) Luciferase expressing 4T1 breast carcinoma (4T1-Luc) were injected into the mammary fat pad of female balb/c mice, (**ii**) 4T1-Luc tumors grew to ~1 cm in diameter, (**iii**) tumors were resected and either UBM or saline implanted in the resection bed, and (**iv**) regrowth at the primary tumor site and lung metastasis occurs. (**B**) Individual tumor growth curves at the primary tumor site and (**C**) survival with saline or UBM. Numerals correspond with steps in (A). (**D**) Representative bioluminescence imaging of 4T1-Luc cells 1 week post resection with UBM or saline implantation. (**E**) Bioluminescence quantification at the primary tumor site and in lung metastases. (N=5, mean ± SE). (**Statistics**) Tumor volume: * $P < 0.05$ UBM. Two-way repeated measures ANOVA with post-hoc Tukey test at each time point before sacrifice. Survival: * $P < 0.05$, log-rank test with the Sidak correction.

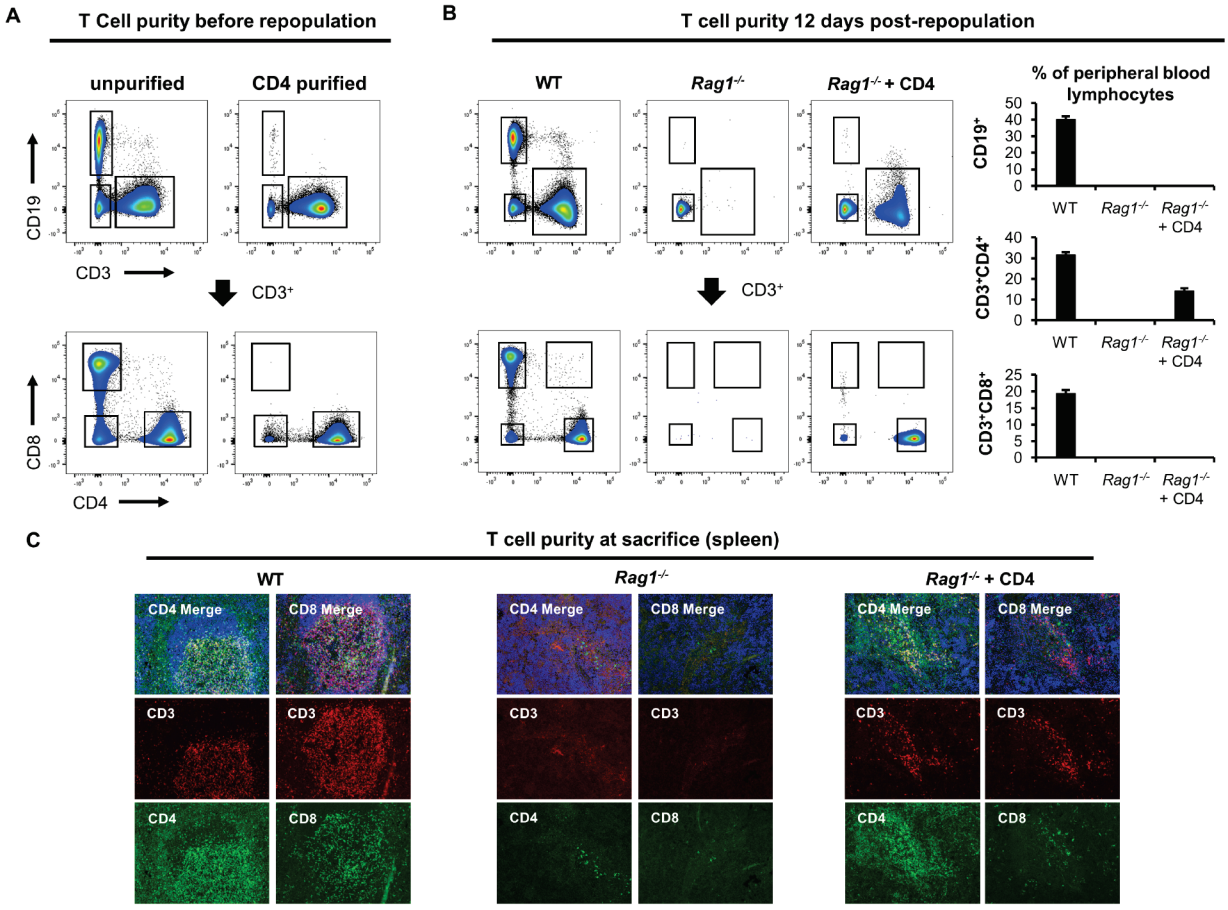

Fig. S3. CD4$^+$ T cell purity in adoptive transfer experiments. (**A**) Flow cytometry was conducted to determine CD4$^+$ T cell purity before (unpurified) and after negative selection from WT mice for use in adoptive transfer experiments. B cells (CD19$^+$), CD4$^+$ T cells (CD3$^+$CD4$^+$), and CD8$^+$ T cells (CD3$^+$CD8$^+$) were evaluated. (**B**) Purified CD4$^+$ T cells were intravenously injected into lymphocyte deficient *Rag1*$^{-/-}$ mice. T cell engraftment and purity was confirmed 12 days later via flow cytometry analysis of peripheral blood and compared to WT and *Rag1*$^{-/-}$ mice. (N=10, mean ± SE, concatenated plots). (**C**) B16-F10 cells were injected into theses mice with and without UBM. When tumors reached the maximum allowable diameter (2 cm), animals were sacrificed and spleens harvested for histologic analysis of T cell purity. CD4$^+$ and CD8$^+$ cells in *Rag1*$^{-/-}$ mice and CD8$^+$ cells in CD4$^+$ T cell repopulated *Rag1*$^{-/-}$ mice were all CD3$^-$ and had a dendritic morphology (N=4-5, representative of 3 fields of view per sample).

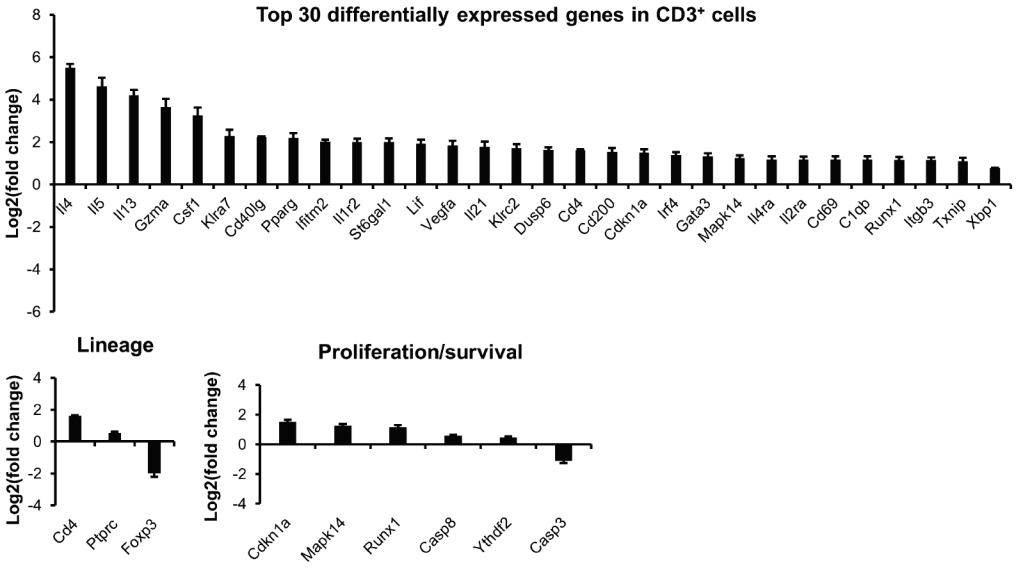

Fig. S4. Differentially expressed genes in T cells sorted from saline and UBM tumors. $CD3^+$ T cells were sorted from UBM and saline delivered tumors for multiplex gene expression analysis using the NanoString platform (accompanying analysis in Fig. 2). The genes with the 30 greatest fold changes with UBM relative to saline delivery 14 days post B16-F10 injection are presented, as well as lineage markers and genes related to regulation proliferation and survival.

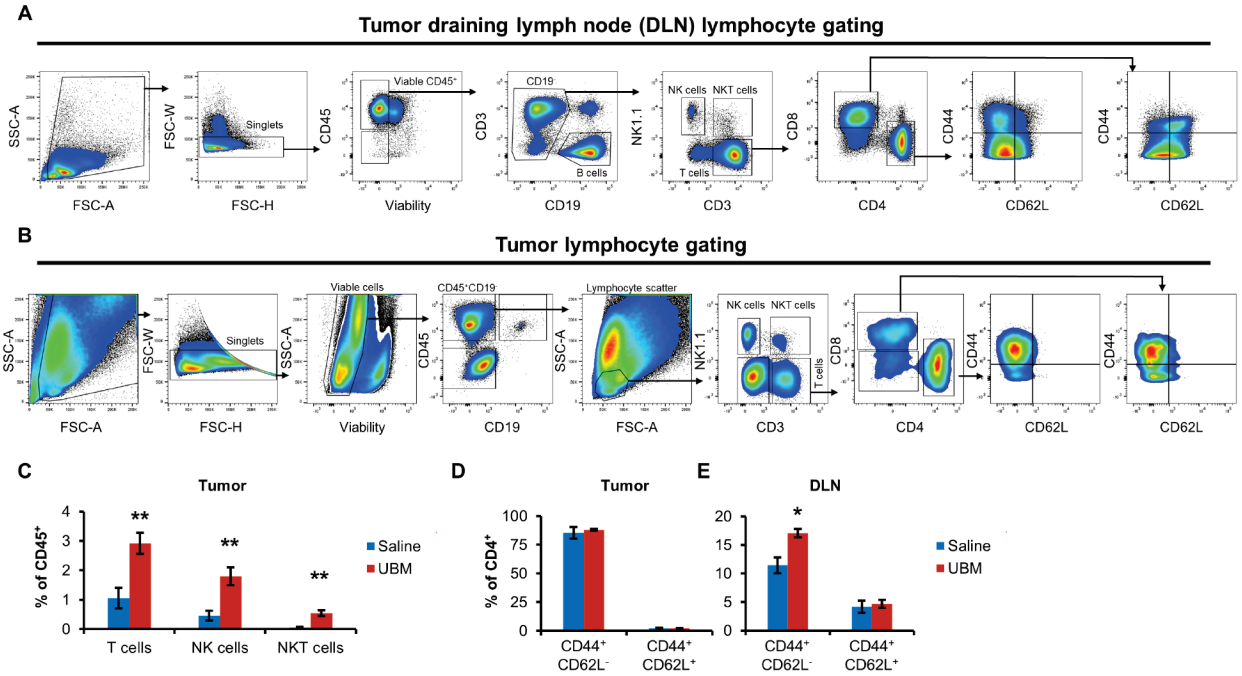

Fig. S5. T lymphocyte characterization in the UBM-tumor microenvironment and DLNs. T cell flow cytometry gating strategy for (**A**) tumor draining lymph nodes and (**B**) tumors when stained for viability, CD45, CD19, CD3, NK1.1, CD4, CD8, CD62L, CD44 (accompanying analysis in Fig. 2). Additional gating steps are included when analyzing tumors to more effectively exclude non-lymphocytes. (**C**) T cells ($CD3^+$), NK cells ($NK1.1^+CD3^-$), and NKT cells ($NK1.1^+CD3^+$) as a percentage of viable $CD45^+$ cells. (**D**) Nearly all tumor infiltrating T cells are antigen experienced ($CD44^+$), while (**E**) UBM delivery increases CD44 expression in tumor draining lymph nodes. (N=5, mean ± SE). **P* < 0.05, ***P* < 0.01 Student's *t* test of saline vs UBM.

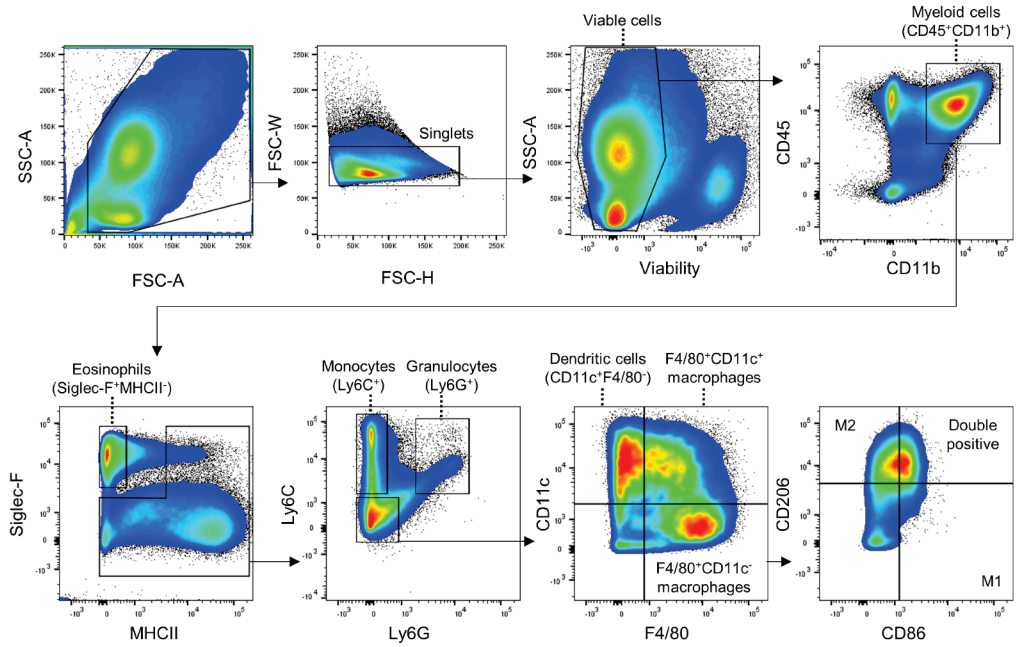

Fig. S6. Gating strategy for myeloid cell analysis with flow cytometry. Myeloid cell flow cytometry gating and marker combinations for each identified cell type (accompanying analysis in Fig. 3). This sample is representative of UBM implantation in WT mice.

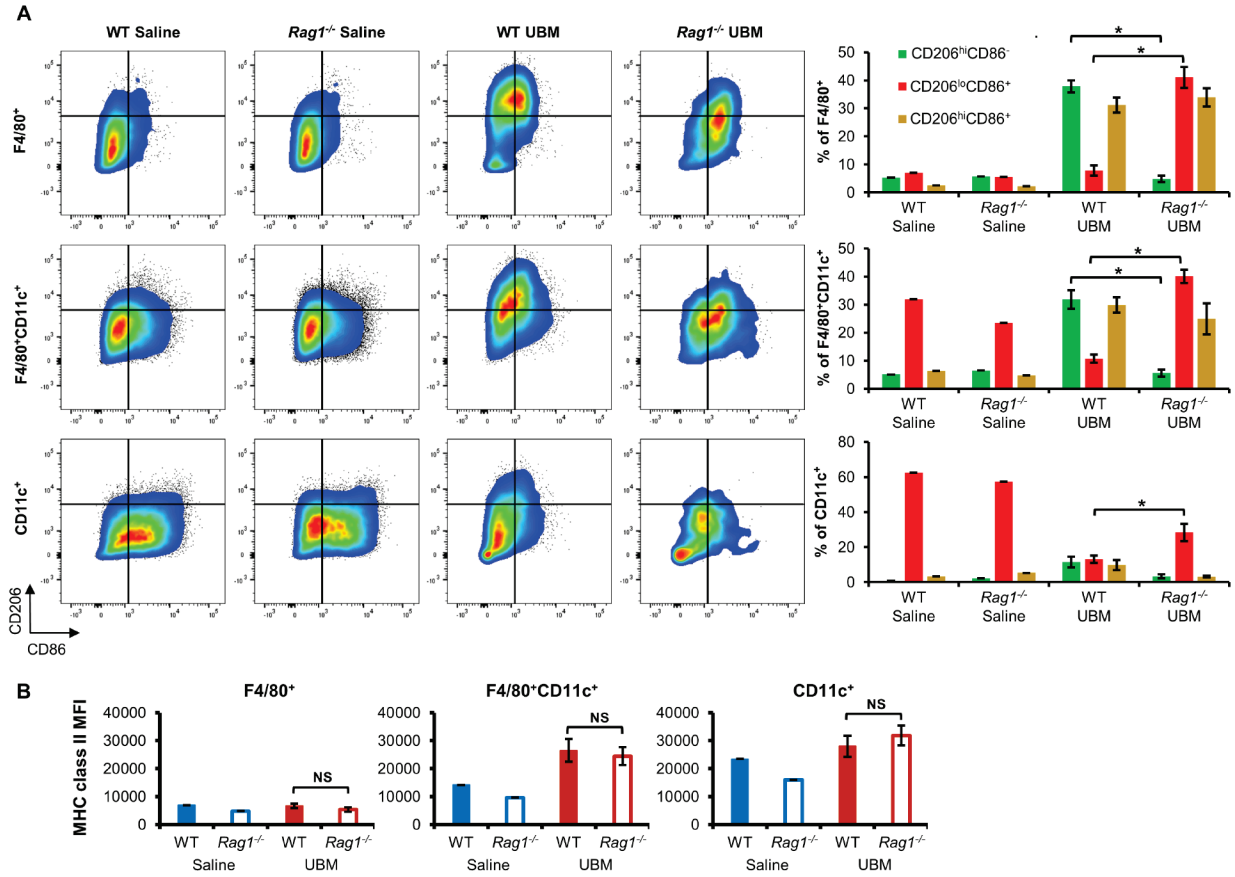

Fig. S7. Detailed analysis of macrophage polarization. (**A**) Macrophage ($F4/80^{+}CD11c^{+/-}$) and dendritic cell ($CD11c^{+}$) populations were analyzed for CD206 (M2 polarization) and CD86 (M1 polarization) expression. The proportion of M2 cells ($CD206^{hi}CD86^{-}$), M1 cells ($CD206^{lo}CD86^{+}$), and double positive cells ($CD206^{+}CD286^{+}$) were quantified for each macrophage population (N=5, mean ± SE). (**B**) Mean fluorescent intensity of major histocompatibility complex II (MHCII) in each macrophage population. (N = 5, mean ± SE). NS, not significant P > 0.05, * $P < 0.05$, ** $P < 0.01$, *** $P < 0.001$ Student's *t* test of WT UBM vs *Rag1*$^{-/-}$ UBM.

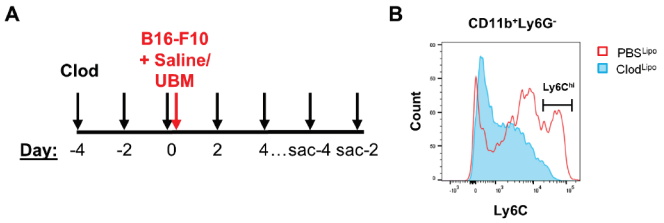

Fig. S8. Macrophage depletion using clodronate liposomes. The role of macrophages in UBM mediated tumor growth inhibition was evaluated by depleting circulating macrophage progenitors with clodronate loaded liposomes. (**A**) Injection schedule for liposome injections, which begin 4 days before UBM and B16-F10 cell implantation and continues every 2 days until sacrifice ("sac"). (**B**) Flow cytometry analysis of peripheral blood to verify a reduction in the number of macrophage progenitors ($CD11b^{+}Ly6G^{-}Ly6C^{hi}$) in clodronate liposome treated animals compared to PBS liposome controls.

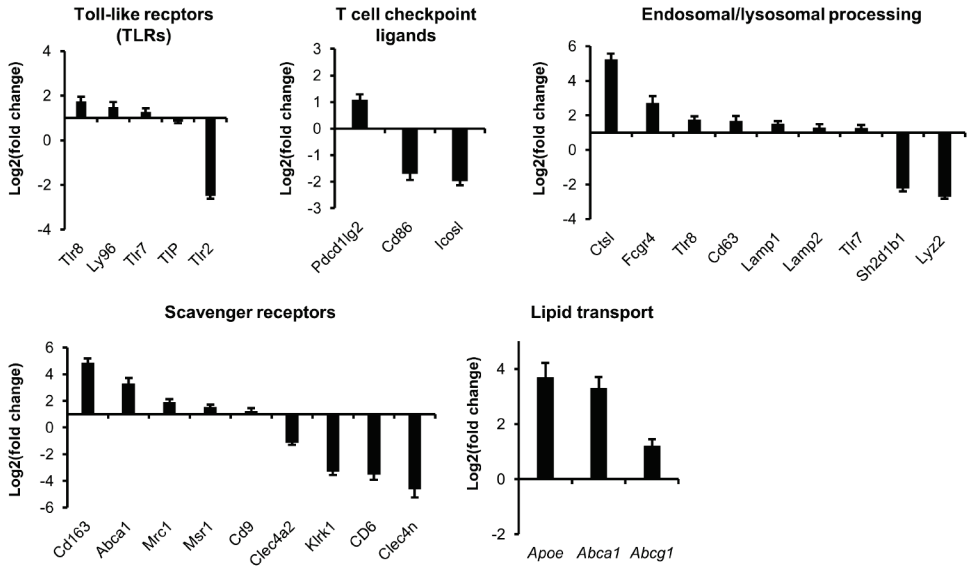

Fig. S9. Differentially expressed genes in macrophages sorted from UBM and saline tumors. F4/80+ cells were sorted from UBM and saline delivered B16-F10 tumors for multiplex gene expression analysis using the NanoString platform (accompanying analysis in Fig. 4). Significantly regulated gene sets with UBM delivery related to: toll like receptors (TLRs), T cell regulation, endosomal and lysosomal activity, scavenger receptors, and lipid transport.

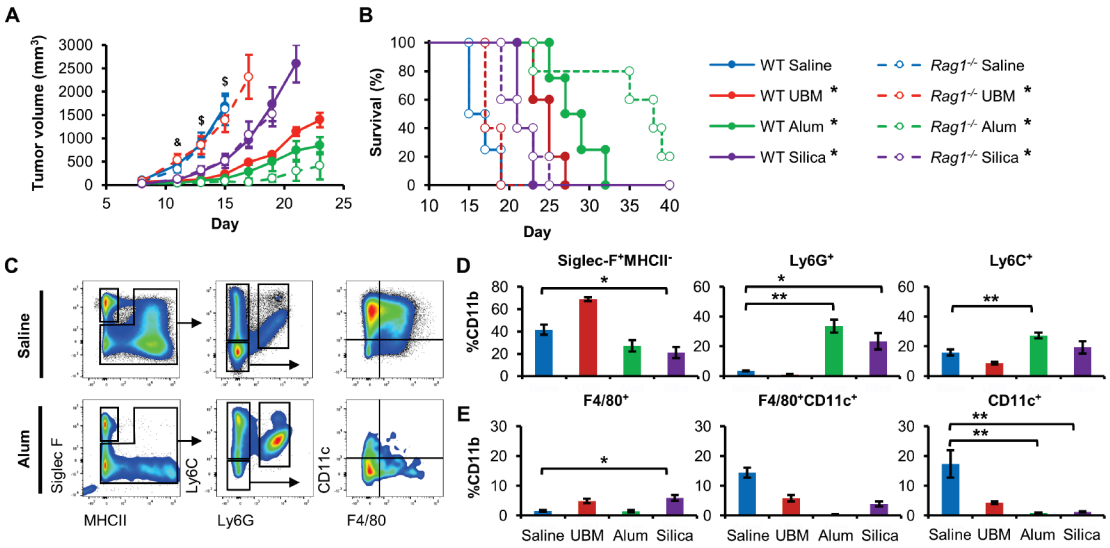

Fig. S10. The synthetic adjuvant material microenvironment is distinct from UBM. B16-F10 tumor growth in the UBM microenvironment was compared to the synthetic adjuvant particulates aluminum hydroxide (alum) and mesoporous silica (silica) in WT and *Rag1*$^{-/-}$ mice. (**A**) Average tumor volume and (**B**) survival were monitored (N = 5, mean ± SE). (**C**) Concatenated flow cytometry plots of myeloid cells isolated from saline (N = 3) and alum (N = 5) 7 days post injection with B16-F10 cells. (**D**) Eosinophil (Siglec-F^{+}MHCII^{-}), granulocyte (Ly6G^{+}), and monocyte (Ly6C^{+}) infiltration 7 days after B16-F10 delivery with saline, UBM, alum, or silica (N = 3 saline, N = 5 alum and silica, N = 5 UBM. UBM data is provided from Fig. 3 as a reference, mean ± SE). (**E**) Macrophage (F4/80^{+}CD11c$^{+/-}$) and dendritic cell (CD11c^{+}) infiltration 7 days after B16-F10 delivery with saline, alum, and silica (N = 3 saline, N = 5 alum and silica, mean ± SE). (**Statistics**) Tumor volume: $ $P < 0.05$ WT saline vs WT UBM, WT alum, WT silica; *Rag1*$^{-/-}$ saline vs *Rag1*$^{-/-}$ alum, *Rag1*$^{-/-}$ silica; WT UBM vs *Rag1*$^{-/-}$ UBM; & $P < 0.05$ WT saline vs WT alum and *Rag1*$^{-/-}$ alum, two-way repeated measures ANOVA with post-hoc Tukey test at each time point before sacrifice. Survival: * $P < 0.05$, log-rank test compared to WT saline with the Sidak correction. Flow cytometry: * $P < 0.05$, ** $P < 0.01$, *** $P < 0.001$ Student's *t* test compared to WT saline (significance indicated indicators in legend).

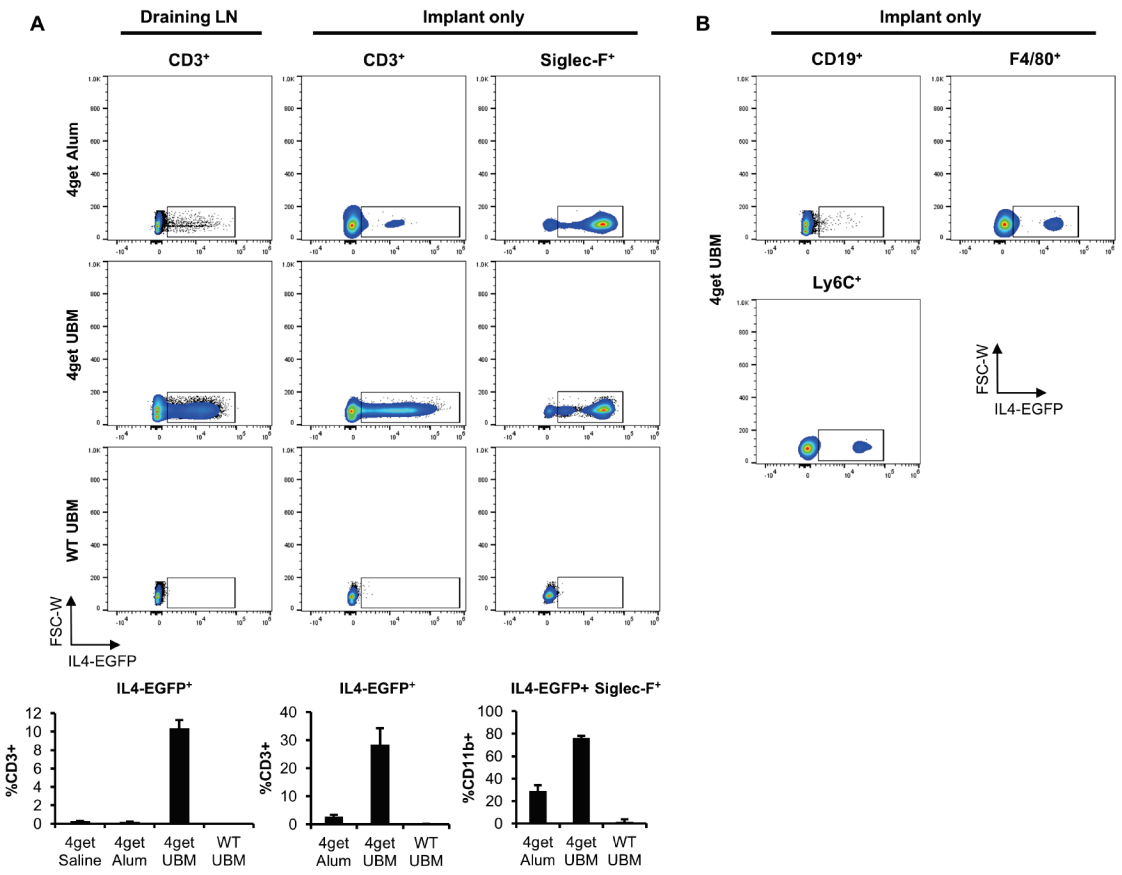

Fig. S11. Acellular UBM induces type 2 immune responses. Acellular UBM, alum, or saline (Implant only without B16-F10 cells) were injected subcutaneously into IL-4-EGFP reporter (4get) or WT balb/c mice. (**A**) T cells ($CD3^+$) in the material draining lymph node and implant, and eosinophils ($Siglec\text{-}F^+$) in the implant were quantified for EGFP expression using flow cytometry. (**B**) B cells ($CD19^+$), macrophages ($F4/80^+$), and monocytes ($Ly6C^+$) expressed relatively little IL-4-EGFP (N = 2 for alum and UBM for each strain, N = 1 for saline, mean ± SD).

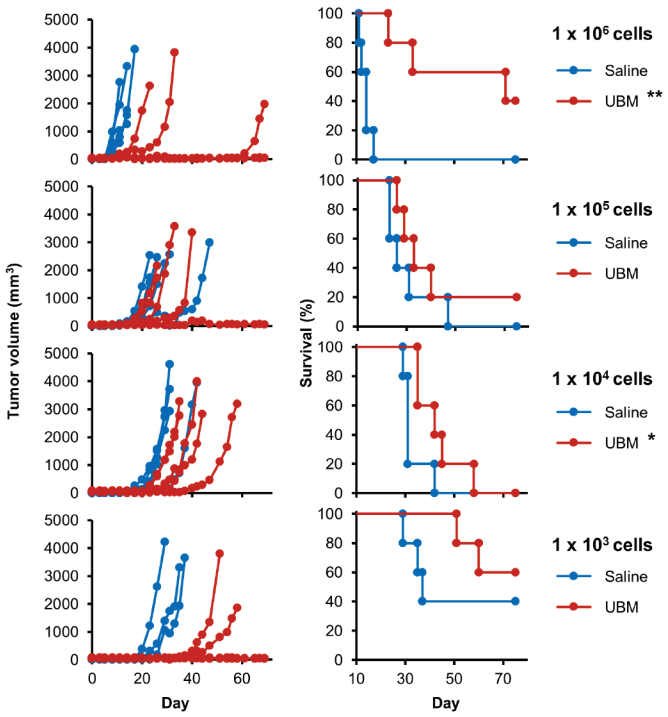

Fig. S12. B16-F10 cell titration with the combination of UBM and anti–PD-1. UBM or saline was co-injected with different doses of B16-F10 cells (10^3-10^6 cells) and treated with anti-PD-1 after 8 days. Individual tumor growth curves and survival for each cell dose (accompanying analysis in Fig. 5). * $P < 0.05$, ** $P < 0.01$ log-rank test compared to saline with the Sidak correction.

A

Material	Cell line (# cells)	Immunotherapy	Figure ref.	Rejected n/total n (%)	Rejection on rechallenge
UBM	CT26 (10^5)	none	Fig 1	1/5 (20%)	Yes
Alum	B16-F10 (10^5)	none	SFig 10	1/5 (20%)	No
UBM	B16-F10 (10^5)	Anti-PD-1	Fig 5	1/10 (10%)	Yes
UBM	B16-F10 (10^5)	IgG Isotype	Fig 5	1/10 (10%)	Partial (delayed to 50 days)
UBM	B16-F10 (10^5)	Anti-PD-1	Fig 5	1/5 (20%)	Yes
Saline	B16-F10 (10^3)	Anti-PD-1	Fig 5	2/5 (40%)	No
UBM	B16-F10 (10^3)	Anti-PD-1	Fig 5	3/5 (60%)	No
UBM	B16-F10 (10^5)	Anti-PD-1	Fig 5	1/5 (20%)	Yes
UBM	B16-F10 (10^6)	Anti-PD-1	Fig 5	2/5 (40%)	Yes

B

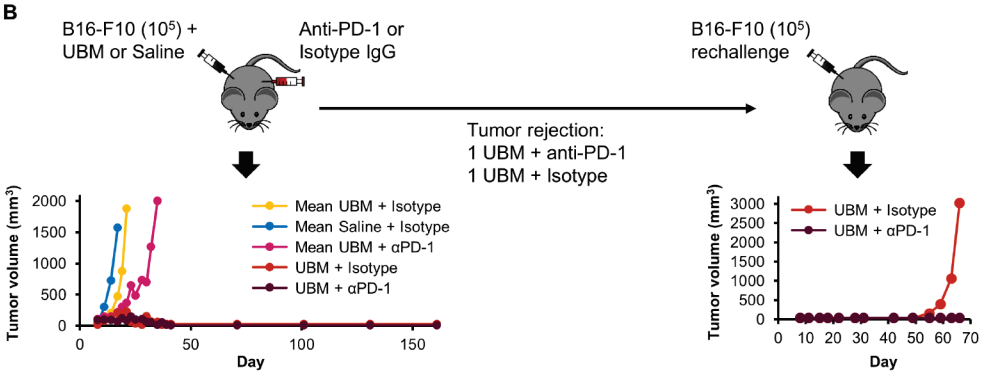

Fig. S13. Tumor rejection occurs in the UBM microenvironment with anti–PD-1 treatment and leads to protection on rechallenge. (**A**) Table summarizing mice that survived the initial cell injection: experimental details, Fig. reference, and whether they rejected the same cell line on rechallenge with 1 x 10^5 cells. (**B**) Schematic and tumor growth of a representative case demonstrating immunological memory on rechallenge. All materials were implanted in WT mice except for alum, which was in *Rag1*$^{-/-}$ mice.

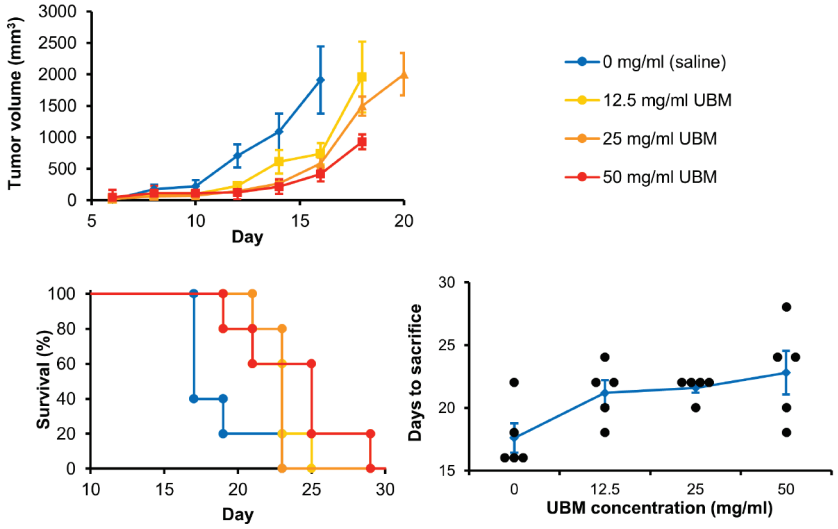

Fig. S14. UBM dose response for tumor growth inhibition. B16-F10 cells and UBM particles were co-injected subcutaneously at 4 different UBM concentrations. Each 100 µl injected contained either 0 mg UBM/ml (saline), 12.5 mg UBM/ml, 25 mg UBM/ml, or 50 mg UBM/ml. Tumor growth and survival was monitored for each concentration (N=5, mean ± SE).

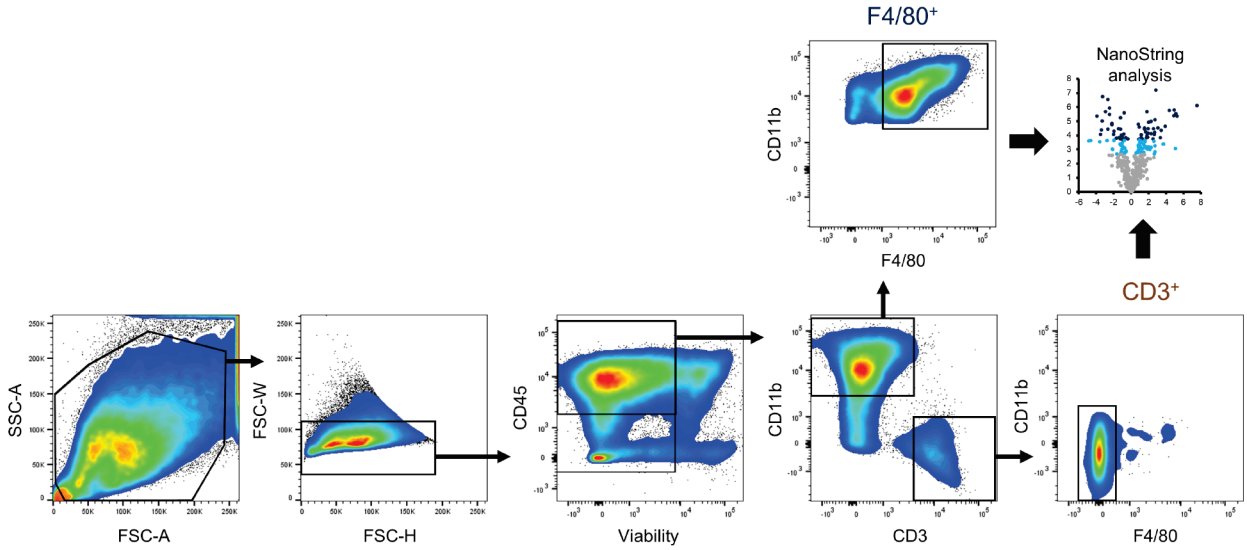

Fig. S15. Gating strategy for T cell and macrophage cell sorting. T cells and macrophages were sorted from UBM and saline delivered tumors for multiplex gene expression analysis.

Table S3. Antibodies used in immunofluorescence histology.

Marker	Species	Clone	Dilution	Manufacturer	Catalog #
CD3	Rabbit	Sp7	1:200	Abcam	ab16669
B220/CD45R	Rat	RA3-6B2	1:400	Biolegend	103202
CD4	Rat	4SM95	1:250	ThermoFisher	14-9766-80
CD8a	Rat	4SM16	1:250	ThermoFisher	14-0195-80
F4/80	Rat	BM8	1:100	Biolegend	123102
Ki67	Rabbit	polyclonal	1:1000	Abcam	ab15580
Fizz1/ RELMα	Rabbit	polyclonal	1 µg/ml	PeproTech	500-P214

Table S4. Antibodies used in flow cytometry experiments.

Marker	Conjugate	Clone	Dilution	Manufacturer	Catalog #
Viability	eFluor780	-	1:1000	ThermoFisher	65-0865-14
Viability	Aqua	-	1:1000	ThermoFisher	L34957
CD45	BV605	30-F11	1:100	Biolegend	103139
CD45	PerCP-Cy5.5	30-F11	1:100	Biolegend	103131
MHC II (I-A/I-E)	AF488	M5/114	1:200	Biolegend	107615
CD11b	AF700	M1/70	1:300	Biolegend	101222
Siglec-F	PE-CF594	E50-2440	1:200	BD biosciences	562757
Ly6C	PerCP-Cy5.5	HK1.4	1:400	Biolegend	128011
Ly6G	Pacific Blue	1A8	1:400	Biolegend	127611
F4/80	PE-Cy7	BM8	1:250	Biolegend	123113
CD11c	APC	N418	1:250	Biolegend	117309
CD206	PE	C068C2	1:250	Biolegend	141705
CD86	BV510	GL-1	1:200	Biolegend	105039
CD3	AF488	17A2	1:150	Biolegend	100212
CD3	APC	17A2	1:150	Biolegend	100235
CD4	PE-Cy7	GK1.5	1:300	Biolegend	100422
CD8	AF700	53-6.7	1:200	Biolegend	100729
FoxP3	Pacific Blue	MF-14	1:150	Biolegend	126409
IL-4	PE	11B11	1:150	Biolegend	504103
IFNγ	BV605	XMG1.2	1:150	Biolegend	505839
IgG1 Isotype	PE	RTK2071	1:150	Biolegend	400407
IgG1 Isotype	BV605	RTK2071	1:150	Biolegend	400433
NK1.1	APC	PK136	1:400	Biolegend	108709
CD44	BV605	IM7	1:200	Biolegend	103047
CD62L	APC-Cy7	MEL-14	1:200	Biolegend	104427
CD19	PE	6D5	1:400	Biolegend	115507
CD16/32	-	9	1:50	Biolegend	101302